# Atmosphere-Ocean modeling exploiting fluid isomorphisms

John Marshall, Alistair Adcroft, Jean-Michel Campin and Chris Hill

Program in Atmospheres, Oceans and Climate,

Department of Earth, Atmospheric and Planetary Sciences

Massachusetts Institute of Technology

December 2002

**Abstract**

We describe how mathematical isomorphisms between the equations that govern the evolution of a compressible atmosphere and an incompressible ocean can be exploited to guide the design of a hydrodynamical kernel that can be used to simulate both fluids.

# List of Figures

# 1 Introduction

The large-scale circulation of the atmosphere and ocean are governed by equations that are remarkably similar to one another because the underlying large-scale fluid dynamics is the same. Yet the development of numerical models of the atmosphere and ocean has occurred almost independently. There has been delayed exchange of ideas developed in one fluid for use in the other. The reasons for this lie largely, we believe, in the sociology of the two disciplines. Atmospheric and oceanic models are developed by different groups of scientists, with different goals and levels of support and who often do not communicate with one another. But the increasing importance of and challenges posed by coupled climate modeling has meant that the need for such collaboration is very urgent.

Here we report on an approach to coupled climate modeling in which the same hydrodynamical algorithm is used to simulate both the atmosphere and

ocean by exploiting isomorphisms between the equations that govern the respective fluids. From one hydrodynamical kernel, separate atmospheric and oceanic models are rendered by use of appropriate physics 'overlaid' on the dynamics, as illustrated schematically in Fig.1. Although the hydrodynamical kernel described has been developed with the express purpose of using it for simulation of both fluids, existing atmospheric/oceanic models could be 'converted' from one to the other.

In section 2 we discuss the theoretical underpinning of our approach. In section 3 we describe the formulation and implementation of the ideas in the MIT hydrodynamical kernel. In section 4 we present illustrations of the kernel in action in studies of both fluids. In section 5 we conclude.

# 2 Atmosphere-Ocean fluid isomorphisms

We begin by simply stating the equations of motion that govern the large-scale atmosphere and ocean in pressure and height coordinates respectively. We will see that these equations are isomorphic: a simple mapping between coordinates and state variables renders complimentary equations. For the purposes of designing a single hydro-dynamical kernel to model both atmosphere and ocean we then go on to write the equations of motion in terms of a generic vertical coordinate, '$r$'.

## 2.1 Pressure coordinate equations for the Atmosphere

The equations representing the evolution of a compressible, hydrostatic atmosphere in pressure coordinates are (see, for example, Haltiner and Williams;1980):

$$\frac{D}{Dt}\overrightarrow{\mathbf{v}}_h + f\overrightarrow{\mathbf{k}} \times \overrightarrow{\mathbf{v}}_h + \nabla_p \Phi = \overrightarrow{\mathcal{F}} \quad (1)$$

$$\frac{\partial \Phi}{\partial p} + \alpha = 0 \quad (2)$$

$$\nabla_p \cdot \overrightarrow{\mathbf{v}}_h + \frac{\partial \omega}{\partial p} = 0 \quad (3)$$

$$\alpha = \frac{\partial \Pi}{\partial p}\theta \quad (4)$$

$$\frac{D}{Dt}\theta = \frac{\mathcal{Q}_\theta}{\Pi} \quad (5)$$

$$\frac{D}{Dt}q = \mathcal{Q}_q \quad (6)$$

where $\overrightarrow{\mathbf{v}}_h = (u, v, 0)$ is the horizontal component of velocity, $\omega = \frac{D}{Dt}p$ is the vertical velocity in pressure coordinates, $f$ is the Coriolis parameter, $\overrightarrow{\mathbf{k}}$ is a unit vector in the vertical, $\Phi = gz$ is the geopotential, $\alpha$ is the specific volume, $T$ is the temperature, $\theta = c_p T/\Pi$ is the potential temperature, $\Pi = c_p \left(\frac{p}{p_o}\right)^\kappa$ is the Exner function, and $q$ is specific humidity. Here $c_p$ is the specific heat at constant pressure, $\kappa = \frac{R}{c_p}$ with $R$ the gas constant and $\frac{D}{Dt} = \frac{\partial}{\partial t} + \overrightarrow{\mathbf{v}}_h \cdot \nabla_p + \omega\frac{\partial}{\partial p}$ is the total derivative in pressure coordinates.

The terms $\overrightarrow{\mathcal{F}}$, $\mathcal{Q}_\theta$ and $\mathcal{Q}_q$ represent sources and sinks of momentum, heat and moisture, respectively, which must be parameterized.

The total energy equation can be formed by taking the dot product of

$\overrightarrow{\mathbf{v}}_h$ with (1), adding $\omega$ times (2) and $\Pi$ times (5) to give:

$$\frac{D}{Dt}\left(\frac{1}{2}|\overrightarrow{\mathbf{v}}_h|^2 + \Phi + \Pi\theta\right) = \overrightarrow{\mathbf{v}}_h \cdot \vec{\mathcal{F}} + \mathcal{Q}_\theta + \partial_t \Phi \tag{7}$$

where $\Pi\theta = c_p T$ is the internal energy[1].

### 2.1.1 Atmospheric Boundary conditions

The boundary conditions at the top and bottom of the atmosphere, shown schematically in Fig.2, are:

$$\begin{aligned} & \omega = 0 \text{ at } p = 0 \text{ (top of the atmosphere)} \\ \omega \quad = \quad & \frac{Dp_s}{Dt}; \text{ at } p = p_s(x,y,t) \text{ (bottom of the atmosphere).} \end{aligned} \tag{8}$$

where $p_s$ is the surface pressure. The boundary condition used on integration of the hydrostatic equation (2) is:

$$\Phi = \Phi_s = gH \text{ at } p = p_s(x,y,t)$$

where $H$ is the height of the mountains at the lower boundary.

The surface pressure evolves according to:

[1] To derive eq(7) we made use of the following relations:

$$\Pi\frac{D}{Dt}\theta = \frac{D}{Dt}(\Pi\theta) - \theta\frac{D}{Dt}\Pi = \frac{D}{Dt}(\Pi\theta) - \theta\partial_p\Pi\frac{D}{Dt}p = \frac{D}{Dt}(\Pi\theta) - \alpha\omega$$

$$\frac{\partial}{\partial t} p_s + \nabla \cdot (p_s \widehat{\mathbf{v}_h}) = 0 \tag{9}$$

where

$$\widehat{\mathbf{v}_h} = \frac{1}{p_s} \int_0^{p_s} \mathbf{v}_h dp.$$

is the $p-$averaged horizontal wind.

## 2.2 Z-coordinate equations for the Ocean

The hydrostatic equations of motion for an incompressible, Boussinesq ocean in height coordinates are:

$$\begin{aligned}
\frac{D}{Dt} \overrightarrow{\mathbf{v}}_h + f \overrightarrow{\mathbf{k}} \times \overrightarrow{\mathbf{v}}_h + \nabla_z \left( \frac{p}{\rho_o} \right) &= \overrightarrow{\mathcal{F}} && (10) \\
\frac{\partial}{\partial z} \left( \frac{p}{\rho_o} \right) + g \frac{\rho}{\rho_o} &= 0 && (11) \\
\nabla_z \cdot \overrightarrow{\mathbf{v}}_h + \partial_z w &= 0 && (12) \\
\rho &= \rho(\theta, S, p) && (13) \\
\frac{D}{Dt} \theta &= \mathcal{Q}_\theta && (14) \\
\frac{D}{Dt} S &= \mathcal{Q}_s && (15)
\end{aligned}$$

where $\overrightarrow{\mathbf{v}}_h = (u, v, 0)$ is the horizontal component of velocity, $w = \frac{D}{Dt} z$ is the vertical velocity, $p$ is the pressure, $\rho(\theta, S, p)$ is the density, $\rho_o$ is a constant reference density, $\theta$ is the potential temperature, $S$ is the salinity and $\frac{D}{Dt} =$

$\frac{\partial}{\partial t} + \overrightarrow{\mathbf{v}}_h \cdot \nabla_z + w\frac{\partial}{\partial z}$ is the total derivative in $z$ coordinates.

The terms $\overrightarrow{\mathcal{F}}$, $\mathcal{Q}_\theta$ and $\mathcal{Q}_q$ represent sources and sinks of momentum, heat and salinity, respectively.

An equation for kinetic energy + potential energy can be formed by taking the dot product of $\rho_o \overrightarrow{\mathbf{v}}_h$ with Eq.(10), adding $\rho_o w$ times Eq.(11) to give:

$$\frac{D}{Dt}\left(\rho_o \frac{1}{2}|\overrightarrow{\mathbf{v}}_h|^2 + g\rho z\right) + \nabla_3 \cdot \left(\overrightarrow{\mathbf{v}}_3 p\right) = \overrightarrow{\mathbf{v}}_h \cdot \vec{\mathcal{F}} + gz\frac{D}{Dt}\rho. \tag{16}$$

The source term in Eq.(16) involving $\frac{D}{Dt}\rho = \left.\frac{\partial\rho}{\partial\theta}\right|_S \mathcal{Q}_\theta + \left.\frac{\partial\rho}{\partial S}\right|_\theta \mathcal{Q}_S + \left.\frac{\partial\rho}{\partial p}\right|_{S,\theta} \frac{D}{Dt}p$ is complicated by the non-linear equation of state. Note that the Boussinesq model approximates total energy by internal energy (Eq.14): the kinetic energy and potential energy, Eq.(16), appear at higher order, independently of the internal energy.

### 2.2.1 Oceanic boundary conditions

The boundary conditions at the top and bottom of the ocean are:

$$\begin{aligned} w &= -\overrightarrow{\mathbf{v}}_h \cdot \nabla H \text{ at } z = -H \text{ (ocean bottom)} \\ w &= \frac{D\eta}{Dt} = -\left(P - E\right) \text{ at } z = \eta \text{ (ocean surface)} \end{aligned} \tag{17}$$

where $P - E$ is precipitation minus evaporation.

The boundary condition used in integration of the hydrostatic equation

is:

$$p = p_s \text{ at } z = \eta$$

where $p_s$ is the pressure exerted by the atmosphere at the ocean's surface.

The surface elevation evolves according to:

$$\frac{\partial}{\partial t}\eta + \nabla \cdot [(H + \eta)\,\widehat{\mathbf{v}_h}] = P - E \tag{18}$$

and

$$\widehat{\mathbf{v}_h} = \frac{1}{(H + \eta)} \int_{-H}^{\eta} \mathbf{v}_h dz.$$

is the depth-averaged horizontal velocity.

## 2.3 The isomorphism

We note that if we simply replace the variables and coordinates in Section 2.1 and 2.2 — set out in Eqs.(1) to (6) and Eqs.(10) to (15) — thus:

$$
\begin{array}{ccc}
ocean & \leftrightarrow & atmos \\
z & \leftrightarrow & p \\
w & \leftrightarrow & \omega \\
\frac{p}{\rho_o} & \leftrightarrow & \Phi \\
g\frac{\rho}{\rho_o} & \leftrightarrow & \alpha \\
S & \leftrightarrow & q \\
\eta & \leftrightarrow & p_s
\end{array}
$$

then we see that equation sets representing atmospheric and oceanic motion are isomorphic - see Fig.4.

It is important to note that the boundary conditions — Eqs.(8) and (17) — and the equations governing the evolution of the 'free surface' in the respective fluids — Eqs.(9) and (18) — are also exactly isomorphic.

## 2.4 General purpose equations in 'r' coordinates

To render atmosphere and ocean models from one dynamical core we exploit the aforementioned 'isomorphisms' between equation sets that govern the evolution of the respective fluids. One system of hydrodynamical equations is written down and encoded in a generic coordinate '$r$'. The model variables have different interpretations depending on whether the atmosphere or ocean is being studied. Thus, for example, the vertical coordinate of our hydrodynamical kernel, '$r$', is interpreted as pressure, $p$, if we are modeling the atmosphere and height, $z$, if we are modeling the ocean - (see Fig.4).

The state of the fluid at any time is characterized by the distribution of velocity $\vec{\mathbf{v}}$, active tracers $\theta$ and $s$, a 'geopotential' $\phi$ and buoyancy $b = b(\theta, s, p)$ which may depend on $\theta$, $s$, and $p$. The equations that govern the evolution of these fields[2] are, written in terms of a generic vertical coordinate, $r$:

$$\frac{D\vec{\mathbf{v}}_h}{Dt} + f\overrightarrow{\mathbf{k}} \times \vec{\mathbf{v}}_h + \boldsymbol{\nabla}_r \phi = \mathcal{F} \tag{19}$$

$$\frac{\partial \phi}{\partial r} - b = 0 \tag{20}$$

$$\boldsymbol{\nabla}_r \cdot \vec{\mathbf{v}}_h + \frac{\partial \dot{r}}{\partial r} = 0 \tag{21}$$

$$b = b(\theta, S, r) \tag{22}$$

$$\frac{D\theta}{Dt} = \mathcal{Q}_\theta \tag{23}$$

$$\frac{Ds}{Dt} = \mathcal{Q}_s \tag{24}$$

Here:

[2]Note that we make the hydrostatic approximation here - isomorphic non-hydrostatic forms are not discussed here.

$r$ is the vertical coordinate

$$\frac{D}{Dt} = \frac{\partial}{\partial t} + \vec{\mathbf{v}}_h \cdot \nabla + \dot{r}\frac{\partial}{\partial r} \tag{25}$$

$\boldsymbol{\nabla} = \boldsymbol{\nabla}_h + \overrightarrow{\mathbf{k}}\frac{\partial}{\partial r}$ is the 'grad' operator

with $\boldsymbol{\nabla}_h$ operating in the horizontal and $\overrightarrow{\mathbf{k}}\frac{\partial}{\partial r}$ operating in the vertical, where $\overrightarrow{\mathbf{k}}$ is a unit vector in the vertical, $t$ is time, $\vec{\mathbf{v}} = (u, v, \dot{r}) = (\vec{\mathbf{v}}_h, \dot{r})$ is the velocity, $\phi$ is the 'pressure'/'geopotential', $f$ is the Coriolis parameter, $b$ is the 'buoyancy', $\theta$ is potential temperature, $s$ is specific humidity in the atmosphere, salinity in the ocean, $\mathcal{F}$'s are forcing and dissipation of $\vec{\mathbf{v}}$, $\mathcal{Q}_\theta$ are forcing and dissipation of $\theta$ and $\mathcal{Q}_s$ are forcing and dissipation of $s$.

The $\mathcal{F}$, $\mathcal{Q}_\theta$ and $\mathcal{Q}_s$ are provided by 'physics' packages that parameterize subgridscale turbulent fluxes in the atmosphere and ocean. The simple parameterizations used to test our modeling approach are described in an appendix.

### 2.4.1 Kinematic Boundary conditions

In discussion of the vertical axis of the model it is useful to distinguish between boundaries which are fixed and boundaries which are moving in our $r$ coordinate - see Fig.4. In the atmosphere where $r \longrightarrow p$ and increases downwards, the upper boundary ($r = 0$) is fixed and the lower boundary

($r = p_s$, the surface pressure) moves. In the ocean where $r \longrightarrow z$ and increases upwards, the lower boundary ($r = -H$, the bathymetry) is fixed and the upper boundary ($r'_s = \eta$, the height of the free surface about its resting position) moves.

**vertical** at bounding $r$ surfaces we set (see Fig.4):

$$\begin{aligned} \dot{r} &= -\vec{\mathbf{v}} \cdot \boldsymbol{\nabla} R_{fixed} \text{ at } r = R_{fixed} \\ \dot{r} &= \frac{Dr_s}{Dt} - P_r \text{ at } r = R_s \end{aligned} \tag{26}$$

where

$$\begin{aligned} R_{fixed} &= -H \text{ at the bottom of the ocean} \\ &= 0 \text{ at the top of the atmosphere} \end{aligned}$$

and

$$R_s = R_o + r'_s$$

where

$$\begin{aligned} R_o &= 0 \text{ at the surface of the ocean} \\ &= R_o(x,y) = p_s^o(x,y) \text{ at the ground} \end{aligned}$$

and

$$\begin{aligned} r_s' &= \eta \text{ at the surface of the ocean} \\ &= p_s' \text{ at the ground.} \end{aligned}$$

and

$$\begin{aligned} P_r &= P - E \text{ at the surface of the ocean} \\ &= 0 \text{ in the atmosphere.} \end{aligned}$$

is the volume mass flux through $r_s$.

Note that $R_s$ is the '$r-$value' of the moving bounding coordinate surface - i.e. the upper surface of the ocean, the bottom surface in the atmosphere. If the fluid is at rest then this bounding coordinate takes on the value $R_o(x,y)$; when the fluid is moving the bounding coordinate moves about this reference by an amount $r_s'$. Thus in the ocean, $R_o = 0; r_s' = \eta$ is the height of the free surface about its resting height, $R_o$, chosen to be zero; in the atmosphere,

$R_o = p_s^o(x,y)$; $r'_s = p'_s$, the fluctuation of the surface pressure about its reference value, $p_s^o(x,y)$;

**horizontal** at lateral boundaries, we suppose that there is no normal flow and impose:

$$\vec{\mathbf{v}} \cdot \vec{\mathbf{n}} = 0$$

where $\vec{\mathbf{n}}$ is the normal to a solid boundary.

### 2.4.2 Atmosphere: '$r = p$'

In the atmosphere - see Figs. 2 and 4 - we interpret:

$$\begin{aligned}
r &= p \text{ as the pressure} && (27)\\
\dot{r} &= \frac{Dp}{Dt} = \omega \text{ as the vertical velocity in } p \text{ coordinates} && (28)\\
\phi &= \Phi = g\,z \text{ as the geopotential height} && (29)\\
b &= -\alpha = -\frac{\partial \Pi}{\partial p}\theta \text{ as the buoyancy} && (30)\\
\theta &= T(\frac{p_c}{p})^{\kappa} \text{ as potential temperature} && (31)\\
s &= q, \text{ as the specific humidity} && (32)
\end{aligned}$$

where $T$ is absolute temperature, $p$ is the pressure, and $z$ is the height of the pressure surface.

At the top of the atmosphere (which is 'fixed' in our $r$ coordinate):

$$R_{fixed} = p_{top} = 0$$

In an atmosphere at rest the pressure at the top of the mountains is given by

$$R_s = R_o(x, y) = p_s^o(x, y)$$

and the geopotential height of the mountains is:

$$\phi = gH_{topo} = \int_{p_s^o}^{1000mb} \alpha_{ref} dp \tag{33}$$

The boundary conditions at top and bottom are given by:

$$\dot{r} = 0 \text{ at } r = p_{top} = 0 \text{ (top of the atmosphere)}$$

$$\dot{r} = \frac{Dr_s}{Dt}; \text{ at } r = R_s = p_s(x, y) \text{ (bottom of the atmosphere)}$$

where $p_s = p_s^o + p_s'$ and $P_r = 0$.

Then Eqs.(19) to (24) yield the set of atmospheric equations in $p$ coordinates, written out in section 2.1.

### 2.4.3 Ocean:'$r = z$'

In the ocean - see Figs.(3) and (4) - we interpret:

$$r = z \text{ as the height} \tag{34}$$

$$\dot{r} = \frac{Dz}{Dt} = w \text{ as the vertical velocity} \tag{35}$$

$$\phi = \frac{p}{\rho_o} \text{ as the pressure} \tag{36}$$

$$b = -g\frac{\rho(\theta, S, r)}{\rho_o} \text{ as the buoyancy} \tag{37}$$

where $\rho_o$ is a fixed reference density of water and $g$ is the acceleration due to gravity.

At the bottom of the ocean:

$$R_{fixed}(x, y) = -H(x, y).$$

At the surface of the ocean:

$$R_s = \eta$$

where $\eta$ is the elevation of the free surface because $R_o = 0$.

The boundary conditions at the top and bottom of the ocean are:

$$\begin{aligned}
\dot{r} &= -\vec{\mathbf{v}} \cdot \boldsymbol{\nabla} R_{fixed} \text{ with } R_{fixed} = -H \text{ (ocean bottom)} \\
\dot{r} &= \frac{Dr_s}{Dt} - P_r \text{ at } r = \eta \text{ (ocean surface) with } P_r = P - E
\end{aligned}$$

Under the above interpretation, Eqs.(19) to (24) yield a consistent set of ocean equations which are written out in $z$ coordinates in section 2.2.

# 3 A hydrodynamical kernel for simulation of the circulation of the atmosphere and ocean

The model we use to step forward Eqs.(19) to (24) - the MITgcm - employs the 'pressure method' comprising prognostic steps for velocity and tracer fields and a diagnostic step to find the pressure field required to maintain non-divergent flow from one timestep to another. Details of the numerical method can be found in Marshall et al (1997a,b). Briefly, we proceed by dividing the total (pressure/geo) potential in to two parts, a surface part, $\phi_s(x, y)$, and a hydrostatic part $\phi_{hyd}(x, y, r)$, and writing the momentum equation in the form

$$\frac{\partial}{\partial t}\vec{\mathbf{v}_h} + \boldsymbol{\nabla}_r \phi_s + \boldsymbol{\nabla}_r \phi_{hyd} = \vec{\mathbf{G}}_{\vec{v}} \tag{38}$$

where $\vec{\mathbf{G}}_{\vec{v}}$ represent advective, Coriolis and stress terms.

Of interest here, in the context of fluid isomorphisms, is the diagnostic step used to obtain hydrostatic and 'surface' pressure fields. This is now described in some detail.

## 3.1 Finding the potential

### 3.1.1 Hydrostatic potential

The hydrostatic pressure field in the interior is obtained by integrating eq.20 w.r.t $r$ from the (moving) $r = R_s$ boundary in to the interior of the fluid to yield:

$$\begin{aligned}
\phi &= \phi_s + \int_r^{R_s} -b dr \\
&= \phi_s + \int_r^{R_o} -b dr + \int_{R_o}^{R_s} -b dr \\
&= \phi_s + \int_r^{R_o} -b dr + \phi_l
\end{aligned}$$

where $\phi_l$ is the $\phi$ at $r = R_o$ due to the load induced by $dr = R_s - R_o$.

The boundary condition applied at $r = R_s$ is:

$$\phi_s = \begin{cases} p_a \text{ at ocean surface} \\ gH \text{ at land surface} \end{cases} \tag{39}$$

Here $p_a$ is the atmospheric pressure (loading) at the surface of the ocean, see Fig.3, (often set to zero) and $gH$ is the geopotential height of the orography

over land defined by Eq.(33).

### 3.1.2 Surface pressure

The surface pressure equation can be obtained by integrating continuity, eq(21), vertically from $r = R_{fixed}$ to $r = R_s$

$$\int_{R_{fixed}}^{R_s} \left( \boldsymbol{\nabla}_r \cdot \vec{\mathbf{v}}_h + \frac{\partial \dot{r}}{\partial r} \right) dr = 0$$

Thus, applying the kinematic boundary conditions, eqs(26), we can write

$$\frac{\partial r_s}{\partial t} + \vec{\mathbf{v}}.\nabla r_s + \int_{R_{fixed}}^{R_s} \boldsymbol{\nabla}_r \cdot \vec{\mathbf{v}}_h dr = P_r$$

where $r_s = R_s - R_o$ is the free-surface $r$-anomaly in units of $r$. Using Leibnitz's theorem, the above can be rearranged to yield:

$$\frac{\partial r_s}{\partial t} + \boldsymbol{\nabla}_h \cdot \int_{R_{fixed}}^{R_s} \vec{\mathbf{v}}_h dr = P_r \tag{40}$$

Eq.(40) is stepped forward in time to yield $r_s$, which has units of '$r$' - the surface pressure in the atmosphere, the free surface height in the ocean.

Finally we note that, to a good approximation

$$\Phi_l \simeq b_s r_s.$$

where $b_s$ is the buoyancy at the surface.

## 3.2 Numerical implementation

In our numerical implementation, rather than adopt terrain following coordinates - for example, $\sigma-$coordinates, the standard approach in meteorology[3] - we use height/pressure as a vertical coordinate and employ partial cells to represent topographic variations, as as described in Adcroft et al (1997) and illustrated in Fig.5.

For clarity, let us specialize eq(40) to the atmosphere by writing it in terms of pressure thus:

$$\frac{\partial p'_s}{\partial t} + \boldsymbol{\nabla}_h \cdot \int_0^{p_s} \vec{\mathbf{v}}_h dr = 0 \tag{41}$$

where

$$p_s = p_s^o + p'_s.$$

Topographic relief is specified through $p_s^o(x, y)$, the pressure over topography in a resting atmosphere. Thereafter, as the fluid evolves, the pressure on topography changes according to Eq.(41) for $p'_s$. We will consider two limit cases:

1. fully non-linear: the integral in Eq.(41) is evaluated over the full range, $0 \longrightarrow p_s^o + p'_s$. However, if $\Delta p'_s$ is a significant fraction of (or larger

[3]Terrain following coordinates introduce considerable complications in the ocean because hydrostatic consistency is very difficult to ensure numerically in the presence of steep slopes and islands - see the discussion in Adcroft et al (1997).

than) $\Delta p$, the vertical discretization of the model, then problems arise due to the possible vanishing of layers.

2. linearized: if Eq.(41) is linearized by evaluating the vertical integral over the range $0 \longrightarrow p_s^o$ then we commit an error of order $\frac{\Delta p_s'}{p_s^o}$ where $\Delta p_s'$ is measure of typical horizontal changes in $p_s'$. Typically, in the atmosphere, $\frac{\Delta p_s'}{p_s^o} \sim \frac{30}{1000} = 0.03$, a rather small number.

# 4 Numerical tests of the isomorphic hydrodynamical kernel

The experiments described here were carried out using the hydrodynamical kernel described in Marshall et al. 1997(a,b) and outlined above - see also http://mitgcm.org. One model is used in all calculations: isomorphisms are used to render atmospheric and oceanic cousins.

## 4.1 The atmosphere

### 4.1.1 Test of the hydrodynamical kernel: Held-Suarez benchmark

The atmospheric isomorph of MITgcm was put through its paces on the cubed sphere, as described in Adcroft et al (2002), with 32x32 grid points per face (C32 - nominally 2.8° resolution). The 'vector-invariant' form of the momentum equations, on which the model is based, supports any orthogonal curvilinear grid, of which the cubed sphere is a convenient choice permitting

uniform gridding and facilitating treatment of polar cap dynamics without the need of a polar filter. The 'dry' model is driven by relaxation to a radiative-convective equilibrium profile, following the description set out in Held and Suarez (1994), designed to test atmospheric hydrodynamical cores. Ten equally spaced levels ($\Delta p = 100$ mb) are used in the vertical. The forcing and boundary layer friction are specified analytically according to Held and Suarez (1994). As in the finite difference model described therein, gridpoint noise is controlled using the eighth-order Shapiro (1970) applied to the wind field.

Figure 6 shows an instantaneous plot of the 500 temperature field. We see cold air over the pole (blue) and warm air along an equatorial band (red). Fully developed baroclinic eddies spawned in the northern hemisphere storm track are evident. There are no mountains or land-sea contrast. In this first calculation a linearized lower boundary condition is used, as described in section 3.2.

Fig.7 shows the 5-year mean, zonally averaged zonal wind. It compares very favorably with the grid-point and spectral models described in Held and Suarez (1994). More detailed comparisons are described in Adcroft et al (2002). Fig.8 shows the difference between the zonal average zonal flow obtained using the linear free surface and the non-linear free surface with ten vertical levels. We see that use of the non-linear free surface introduces changes of only $\sim 1ms^{-1}$.

### 4.1.2 The atmospheric model with 'physics'

To further demonstrate how our isomorphed model works in practice we examine the climatology of an atmospheric version of the model (which we call AIM, for Atmosphere of Intermediate Complexity) obtained by "plugging in" - see Fig.(1) - the atmospheric package developed by Molteni (2002) in to our dynamical core with 5 vertical levels at C32 on the cubed sphere. The topography is represented using 'partial cells', as described in Adcroft et al (1997) and a linearized treatment of Eq.(40) is employed. This example serves as a "proof of concept". The model physics (christened SPEEDY by Molteni, 2002, are briefly described in an appendix) are of intermediate complexity and intended to be used in extended coupled climate integrations for studies of predictability and paleo-climate. Despite the idealized nature of the model 'physics' and its crude vertical structure, we shall see that the model exhibits considerable realism.

In the experiment described here, AIM is configured with five vertical levels (at 75, 250, 500, 775, and 950 mb) one in the stratosphere, three in the free troposphere and one in the planetary boundary layer, as in the model described in Molteni (2002). Monthly-mean global sea surface temperature, land temperature, soil moisture and surface albedo are prescribed.

Fig.9 compares the model's zonal average $T$ climatology with analyzed fields from NCEP. We see that errors are less than $2°C$ in the middle to lower troposphere, rising to $8°C$ at the level of the jet maxima. Fig. 10 compares the zonal average zonal wind with analyzed fields. The jet-streams

are of reasonable strength but the trade-wind belt is somewhat weak in the troposphere.

Modeled anomalies in the height of the 500mb surface in DJF is compared with the observations in Fig.11. The pattern of variability is broadly consistent with observations, but with considerably reduced amplitude. Fig.12 compares the modeled annual mean air-sea heat flux with observations. We observe similar patterns and amplitude of flux.

Before going on to describe results using our ocean isomorph, we have also compared a wide variety of fields from our simplified model with that of Molteni (2002) - who used his 'SPEEDY' physics package with the GFDL dynamical core - and find very similar results.

## 4.2 Ocean

To illustrate the application of the hydrodynamical kernel configured for the ocean, Figs.13, 14 and 15 shows a numerical solution on exactly the same cubed grid as the atmospheric model, C32. The model is configured with 30 levels in the vertical with a maximum depth of 6000 m, forced with monthly wind stress from (Trenberth et al, 1989), monthly observed heat and fresh water fluxes (Jiang et al, 1999), and with a restoring of sea surface temperature to monthly climatology (Levitus, 1994). The restoring time-scale of 12 days for a top layer thickness of 10 m corresponds to 40 $\mathrm{Wm^{-2}K^{-1}}$. The model parameters are listed in table 1 of the appendix. The bathymetry was generated from the ETOPO5 world bathymetry using a topology preserving

algorithm described in Adcroft et al (2002).

Fig.13 shows the sea surface height at equilibrium after 5000 years of integration and reveals the surface expression of the major ocean gyres and the circumpolar current. The flow at a depth of 2km, together with the salinity field, Fig.14, shows salty North Atlantic Deep Water flowing south along the western boundary of the Atlantic Basin to join circumpolar deep flow. The global overturning streamfunction is plotted in Fig.15 showing downwelling at the northern polar regions and upwelling around Antarctica.

# 5 Conclusions

We have described how mathematical isomorphisms between the equations that govern the atmosphere and ocean can be exploited to design a single hydrodynamical core that can be used to simulate both fluids. Our approach has been illustrated by 'plugging in' physics packages to the hydrodynamical core of the MITgcm to render atmospheric and oceanic models of intermediate complexity. Although MITgcm has been designed specifically with the isomorphism in mind, we believe that existing atmospheric[4] (oceanic) cores could be modified to yield an the oceanic (atmospheric) counterpart.

The advantages of the approach outlined here are considerable:

1. algorithmic developments of the core hydrodynamics are inherited by both atmosphere and ocean with no extra cost.

[4]The exception would be atmospheric cores based on spectral techniques which cannot be easily modified to describe fluid flow in ocean basins.

2. working on a common core brings atmospheric and oceanic modelers together and breaks down artificial barriers between them.

3. parallelization of forward hydrodynamics and its differentiation to yield tangent linear and adjoint models is automatically inherited by both components of the coupled climate system.

4. coupling of atmospheric and oceanic models is inherently simpler and more logical because the two models use the same grid.

Recent examples of model developments driven by applications in one fluid finding immediate application in the other, made possible (and straightforward) by the isomorphism, are:

1. the cubed sphere of Adcroft et al (2002), developed for applications in meteorology, has obvious advantages in the ocean too, with improved treatment of polar cap, ice dynamics and avoidance of polar filters to lengthen the timestep.

2. studies of the importance of the Boussinesq approximation in ocean modeling. As described in de Szoeke and Samelson (2002), non-Boussinesq effects in ocean models can be elegantly taken in to account by adopting pressure as a vertical coordinate. The $z \longleftrightarrow p$ isomorphism outlined here can be readily used to switch between $z-$coordinate ocean models and $p-$coordinate ocean models - see Losch et al. (2002) where the MITgcm isomorphic kernel is used in this manner.

One serious complication of the isomorphic approach put forward here lies in the treatment of the boundary conditions - see Section 3.1.2 and 3.2. Since Phillips (1957), the common approach in meteorology has been to adopt sigma coordinates ($\sigma = \frac{p}{p_s}$), mapping the vertical coordinates on to $0 \rightarrow 1$. Use of $\sigma$ coordinates in the ocean introduces significant problems in the presence of islands and steep topographic slopes - see, for example, the discussion in Adcroft et al.(1997). If a pure $p-$coordinate is used (as in the examples shown here) then if surface pressure fluctuations are a considerable fraction of, or larger than, the interval used to discretize pressure in the vertical, then special measures have to be taken if the boundary conditions are to be treated accurately. These will be reported in a forthcoming paper.

# 6 Acknowledgements

This work would not have been possible without support from ECCO and MIT's Climate Modeling Initiative.

# 7 References

Adcroft, A.J., Hill, C.N. and J. Marshall, (1997) Representation of topography by shaved cells in a height coordinate ocean model. Mon Wea Rev, vol 125, 2293-2315

Adcroft, A., J-M. Campin, C. Hill and J. Marshall (2002): Implementation of an atmosphere-ocean general circulation model on the expanded spherical cube. submitted to Mon. Wea. Rev.

Brugge, R.H., Jones, H. and J. Marshall (1991). Non-hydrostatic modeling for studies of open-ocean deep convection. Deep Copnvection and Deep Water Formation in the Ocean. P.C. Chu and J.G. Gascard, Eds., vol 57 of Elsevier Oceanogr. Ser., Elsevier Sci., pp 325-240

de Szoeke, R.A. and R. M. Samelson (2002) The duality between the Boussinesq and Non-Boussinedq hydrostatic equations of motion. J. Phys. Oceanogr., 32(8), 2194-2203

Gent and McWilliams (1990) Isopycnal mixing in ocean circulation models. J. Phys. Oceanogr. 20(1): 150-155

Haltiner, G. and R. Williams (1980) Numerical Prediction and Dynamic Meteorology, 2nd Edition, Wiley

Held, I. and M. Suarez A (1994) A proposal for the intercomparison of the dynamical cores of atmospheric general circulation models; BAMS, 75 (10): 1825-1830

Jiang, S., P. Stone and P. Malanotte-Rizzoli (1999) An assessment of the GFDL ocean model at couarse resolution: Annual-mean climatology. J. Geophys.Res., 104, 25623-25645

Levitus, S. (1994) World Ocean Atlas. National Ocean Data Center.

Losch, M., Adcroft, A. and J-M. Campin (2002) How sensitive are general circulation ocean models to the Boussinesq approximation? Submitted.

Marshall, J., C. Hill, L. Perelman, and A. Adcroft, (1997a) Hydrostatic, quasi-hydrostatic, and nonhydrostatic ocean modeling. J. Geophysical Res., 102(C3), 5733-5752.

Marshall, J., A. Adcroft, C. Hill, L. Perelman, and C. Heisey, (1997b) A finite-volume, incompressible Navier Stokes model for studies of the ocean on parallel computers, J. Geophysical Res., 102(C3), 5753-5766.

Molteni, F. (2002) Atmospheric simulations using a GCM with simplified physical parameterizations. I: Model climatology and variability in multi-decadal experiments.

Phillips, N.A., (1957) A coordinate system having some special advantages for numerical forecasting. J. Meteor. 14. p184.

Trenberth, K., J. Olson, and W. Large: (1989) A global ocean wind-stress climatology based on ECMWF analyses. Technical Report NCAR/TN-338+STR, NCAR, Boulder, Colorado.

# 8 Appendix

The distinguishing difference between the atmosphere and the ocean systems is not the dynamics, but rather the source terms that appear on the right hand sides of Eqs.(1) to (6) and Eqs.(10) to (15) which represent distinct physical processes. To accommodate different physical processes in the two fluids we have constructed component software packages that can be easily switched in and out, as represented schematically in Fig.1. Substitution of

the ocean physics package by an atmospheric physics package is all that is required to transform the model from an atmospheric to an ocean.

## 8.1 Atmospheric Package

The physics package developed by Molteni (2002) is well suited to exploratory climate simulation. It is sufficiently concise that a single person can grasp it in its entirety but, as illustrated in section 4, exhibits considerable realism. The atmospheric physics package, described in detail in Molteni (2002), is based on the same physical principles as 'state of the art' models. It utilizes the following limited set of modules parameterizing key processes:

**Surface fluxes of momentum and energy** Fluxes are defined by bulk aerodynamic formulae with different exchange coefficients between land and sea. Coefficients for (sensible and latent) heat fluxes also depend on the vertical gradient of potential temperature between the surface and the lowest model level.

**Convection** A simplified mass-flux scheme is activated when conditional instability is present (namely, where saturation moist static energy decreases with height between the planetary boundary layer (PBL) and the two upper-tropospheric layers), and where relative humidity in the PBL exceeds a fixed threshold. The cloud-base mass flux (at the top of the PBL) is such that the PBL relative humidity is relaxed towards the threshold value. Detrainment occurs only at the cloud-top level (determined by the conditional instability criterion), while entrainment occurs in the lower troposphere if the cloud top

is at the highest tropospheric level. The air in the updrafts is assumed to be saturated.

**Large-scale condensation** When relative humidity exceeds a fixed threshold, specific humidity is relaxed towards the corresponding threshold value, and the latent heat content removed from the atmosphere is converted into dry static energy.

**Cloud cover** Cloud cover is determined diagnostically from the maximum relative humidity in an air column including all tropospheric layers except the PBL.

**Short-wave radiation** SW radiation is reflected by clouds at the top of the troposphere and at the surface; the cloud albedo is proportional to the total cloud cover. SW transmissivity is a function of layer mass, specific humidity and cloud cover.

**Long-wave radiation** A four-band LW scheme is used, one for the atmospheric 'window' and the remaining four for the absorption by water vapor and carbon dioxide, dependent on the mass and humidity of the layers.

**Vertical diffusion (shallow convection)** Vertical diffusion only acts between the two lowest model layers. Dry static energy and specific humidity are diffused when a conditional instability criterion is satisfied. Otherwise, only humidity is diffused, at a slower rate.

| | |
|---|---|
| Horizontal eddy viscosity, $A_h$ | $3 \times 10^5$ m$^2$ s$^{-1}$ |
| Vertical eddy viscosity, $A_v$ | $1.67 \times 10^{-3}$ m$^2$ s$^{-1}$ |
| Bottom drag coefficient, $C_D$ | $1 \times 10^{-3}$ s$^{-1}$ |
| Isopycnal/thickness eddy diffusion, $\kappa_{GM}$ | $10^3$ m$^2$ s$^{-1}$ |
| Vertical eddy diffusion, $\kappa_v$ | $5 \times 10^{-5}$ m$^2$ s$^{-1}$ |
| Enhanced mixing (convection), $\kappa_c$ | 10 m$^2$ s$^{-1}$ |
| Reference density, $\rho_o$ | 1035 kg m$^{-3}$ |
| Level thickness, $\Delta z$ (m) | 10 10 15 21 28 36 45 55 66 78 |
| | 91 105 120 136 154 172 191 211 232 254 |
| | 278 302 327 353 380 408 437 466 497 529 |

Table 1: Parameters used in the ocean circulation experiment.

## 8.2 Ocean Package

The oceanic counterparts to the atmospheric physics have been extracted from our core ocean model - see Marshall et al (1997a,b) and http://mitgcm.org. Components that represent ocean-only processes employed in the calculations described here are:

**Convective adjustment** Statically unstable fluid parcels are homogenized through adjustment or through implicit vertical diffusion.

**Geostrophic Eddy Parameterisation** Following Gent and McWilliams (1990), tracers are advected by the 'Transformed Eulerian Mean' (TEM), expressed as a function of the heat flux by unresolved baroclinic instability, parameterised as a flux down the large-scale temperature gradient. TEM is used together with an along-isopycnal diffusion of tracers.

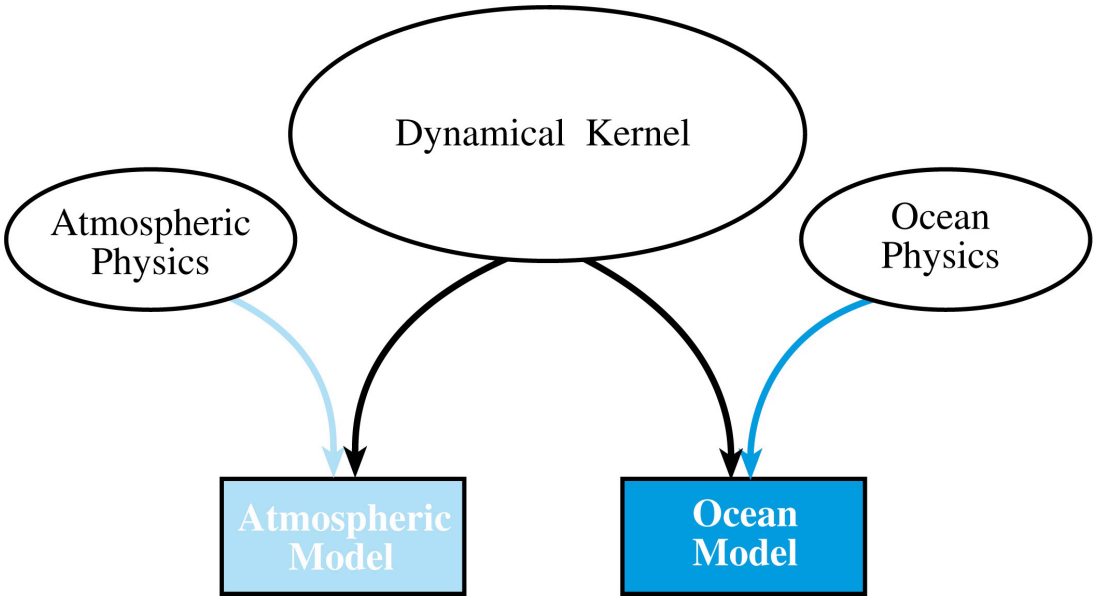


Figure 1: A single dynamical kernel is used to drive forward both oceanic or atmospheric models.

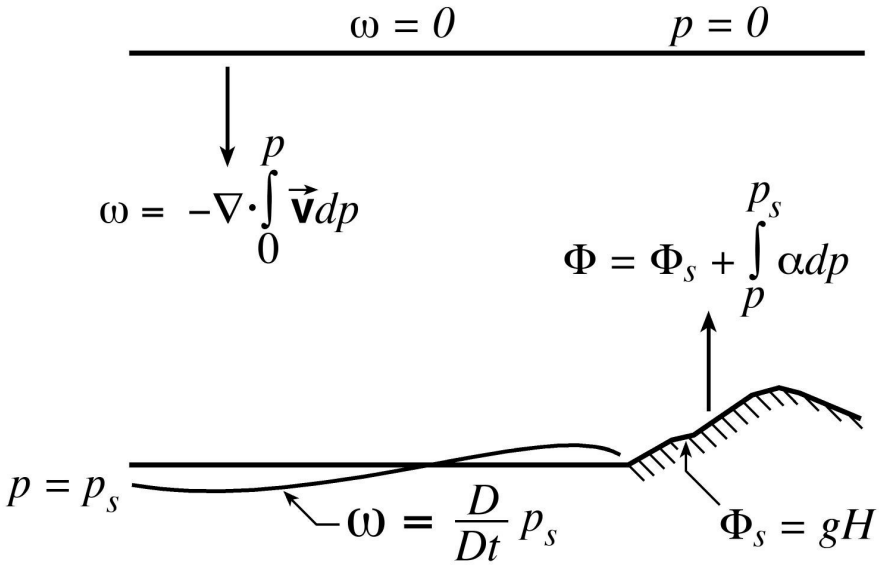


Figure 2: The vertical structure of the atmospheric model. The hydrosatic equation is integrated up from the lower boundary to yield geopotential height, the continuity down from the upper boundary to yield vertical velocity.

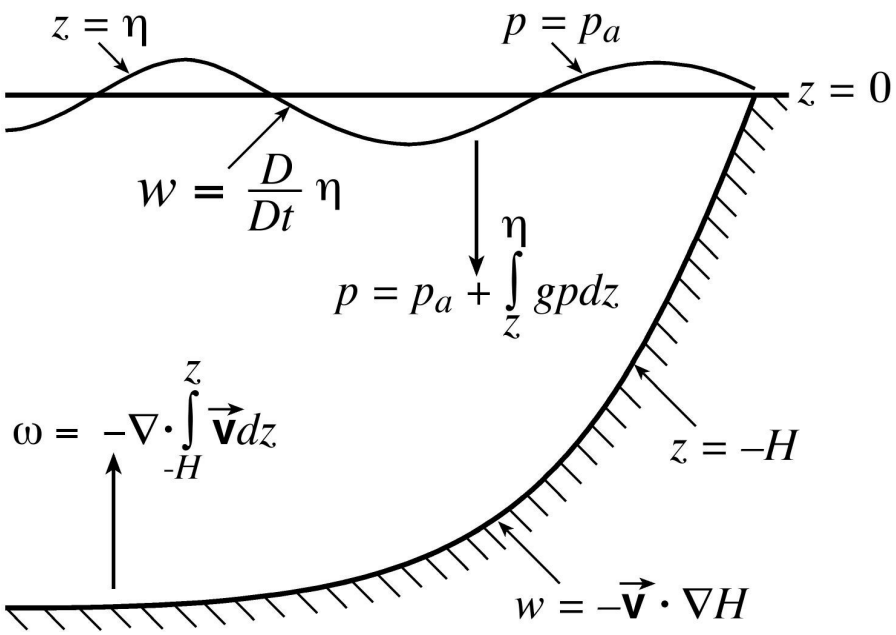


Figure 3: The vertical structure of the ocean model. The hydrostatic equation is integrated down from the surface to yield the pressure field: the continuity equation up from the bottom to yield the vertical velocity.

The equations in 'r' coordinates

$$\frac{D\vec{\mathbf{v}}_h}{Dt} + f\mathbf{k}\times\vec{\mathbf{v}}_h + \nabla_r\phi = \vec{\mathcal{F}}$$

$$\frac{\partial\phi}{\partial r} - b = 0$$

$$\nabla_r \cdot \vec{\mathbf{v}}_h + \frac{\partial\dot{r}}{\partial r} = 0$$

$$b = b(\theta, s, r)$$

$$\frac{D\theta}{Dt} = \mathcal{Q}_\theta$$

$$\frac{Ds}{Dt} = \mathcal{Q}_s$$

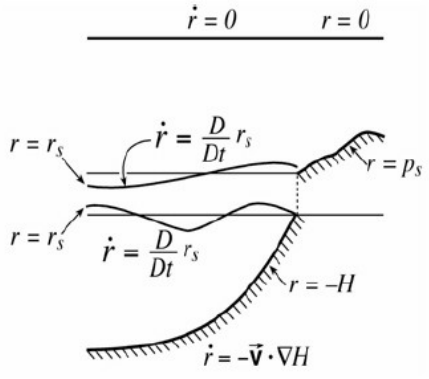


Boundary conditions

$$\frac{\partial r_s}{\partial t} + \nabla_h \cdot \int_{R_{fixed}}^{R_s} \vec{\mathbf{v}}_h dr = P_r$$

$$\dot{r} = -\vec{\mathbf{v}} \cdot \nabla R_{fixed} \text{ at } r = R_{fixed}$$

$$\dot{r} = \frac{Dr_s}{Dt} - P_r \text{ at } r = R_s$$

| *ocean* | | | | *atmos* |
|---|---|---|---|---|
| $z$ | $\leftarrow$ | $r$ | $\rightarrow$ | $p$ |
| $w$ | $\leftarrow$ | $\dot{r}$ | $\rightarrow$ | $\omega$ |
| $\frac{p}{\rho_o}$ | $\leftarrow$ | $\phi$ | $\rightarrow$ | $\Phi$ |
| $-g\frac{\rho}{\rho_o}$ | $\leftarrow$ | $b$ | $\rightarrow$ | $-\alpha$ |
| $\theta$ | $\leftarrow$ | $\theta$ | $\rightarrow$ | $\theta$ |
| $S$ | $\leftarrow$ | $s$ | $\rightarrow$ | $q$ |
| $\eta$ | $\leftarrow$ | $r_s'$ | $\rightarrow$ | $p_s'$ |
| $P-E$ | $\leftarrow$ | $P_r$ | $\rightarrow$ | 0 |

Figure 4: The atmosphere and ocean rendered in terms of the '$r$' coordinate.

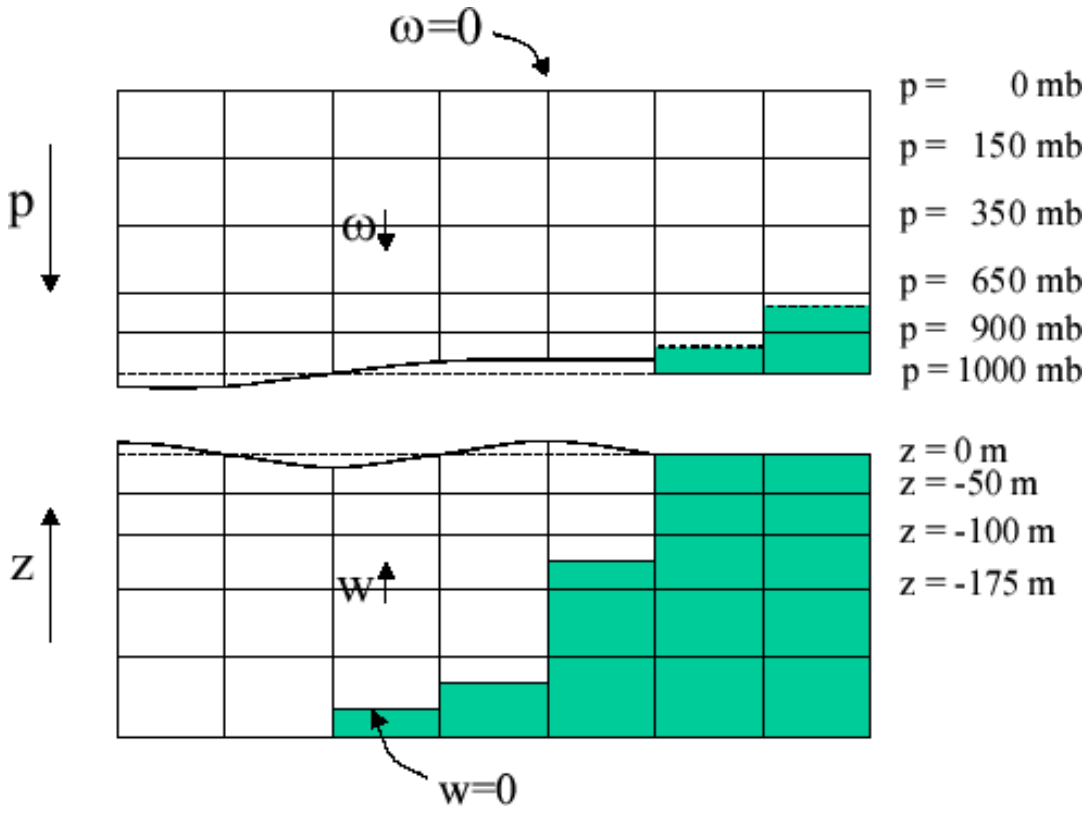


Figure 5: The isomorphism in the discrete model. In the MITgcm partial cells are used to represent orography/bathymetry.

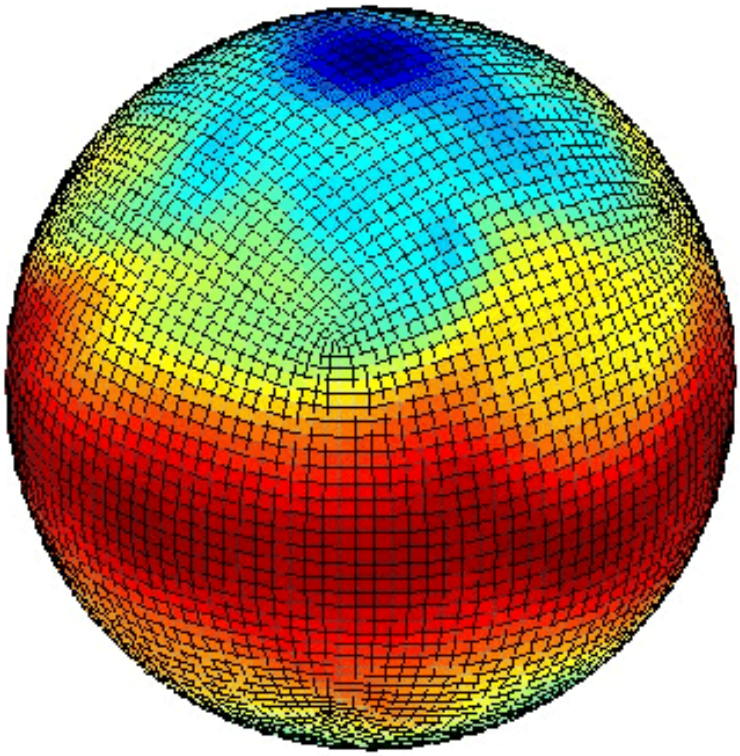

Figure 6: Instantaneous plot of the temerature field at 500mb obtained using the atmospheric isomorph of MITgcm on the cubed sphere at C32. The projection of the sphere on to the cube can be clearly discerned.

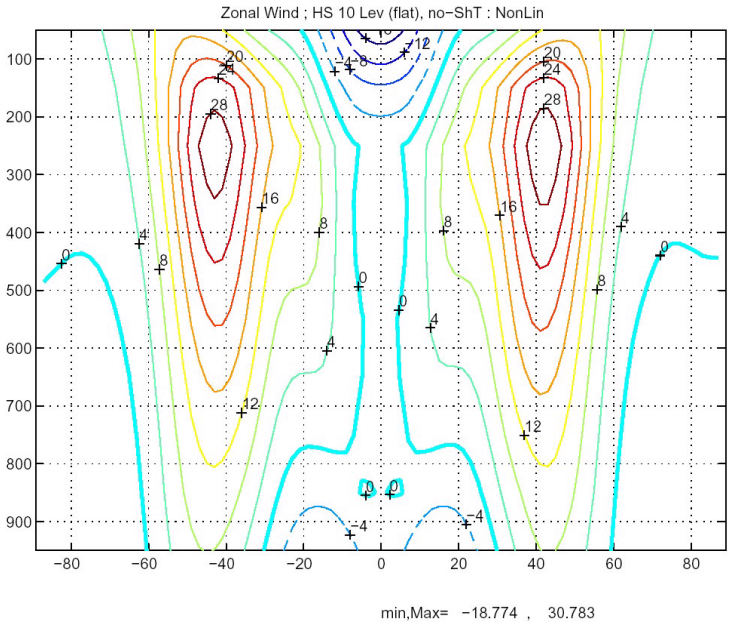


Figure 7: Five year mean, zonally averaged zonal flow from a cube-sphere simulation using Held-Suarez forcing with 10 vertical levels. The flow compares very favorably to that published in Held and Suarez (1994). The c.i.= $4ms^{-1}$.

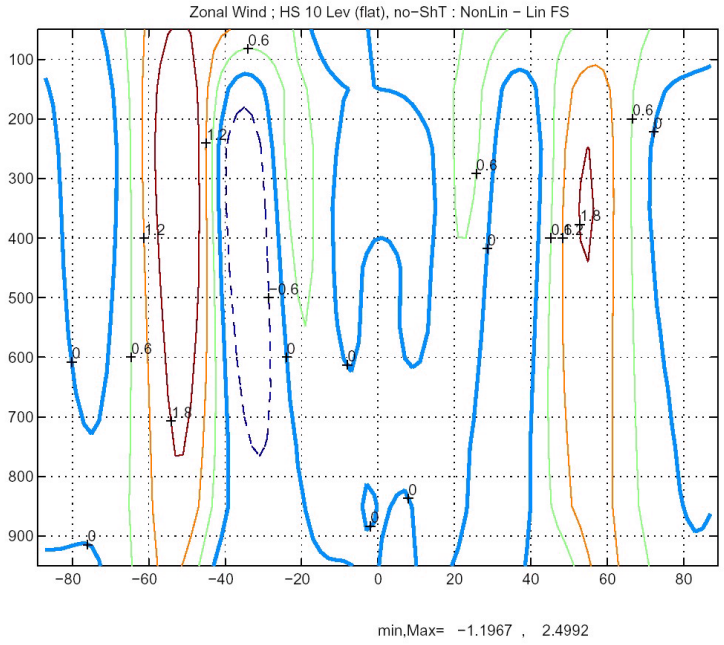


Figure 8: The difference between the zonal average zonal flow obtained using a linear free surface - see Fig.7 - and a non-linear free surface. On the cubed sphere at C32 with ten vertical levels. The c.i.= $0.6ms^{-1}$

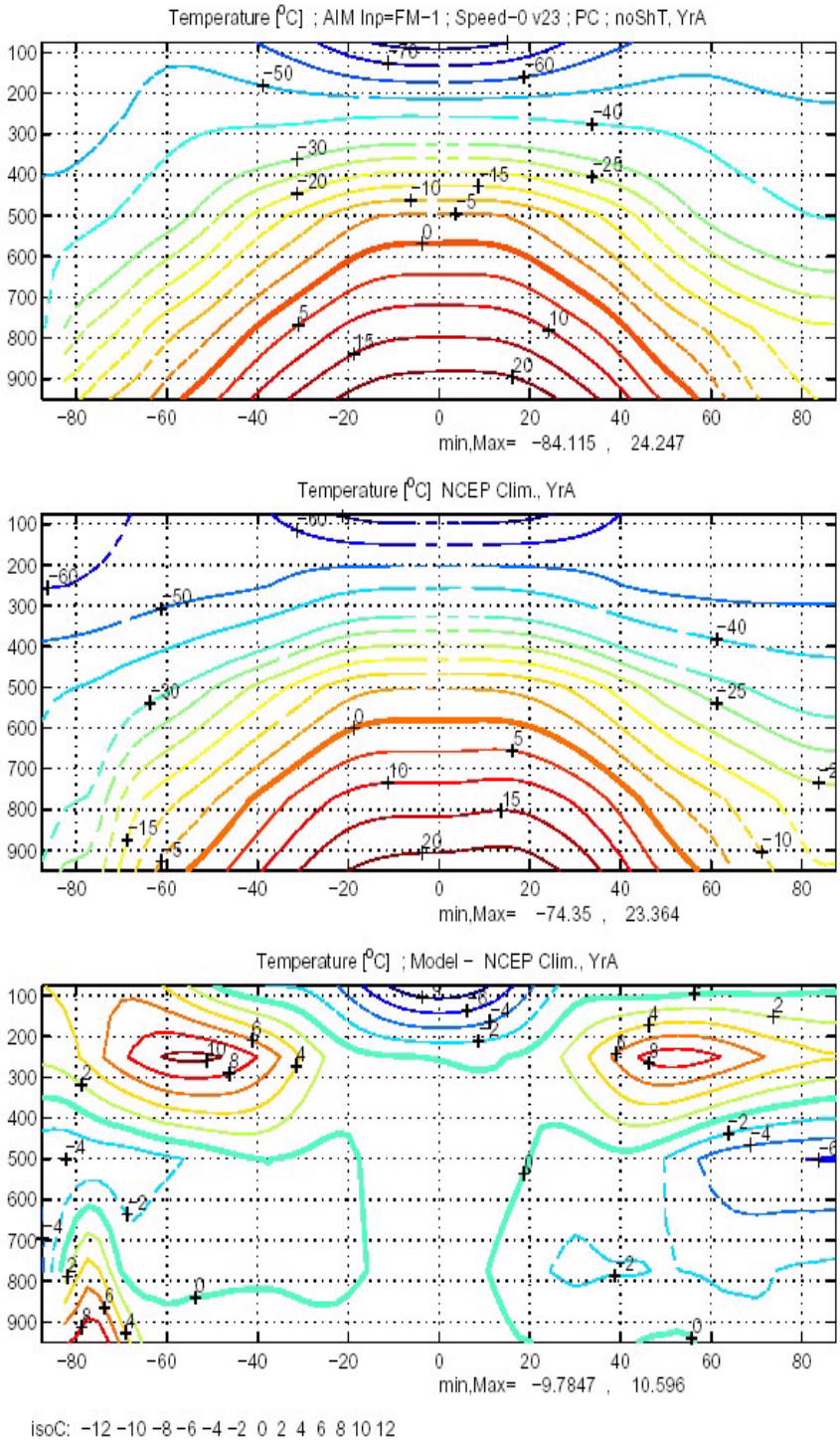




Figure 9: The zonal-average annual mean $T$ field obtained from a 5 year integration of the model (top) compared to the NCEP reanalysis (middle) and 'model' minus ''analysis' (bottom): c.i.= $2°C$.

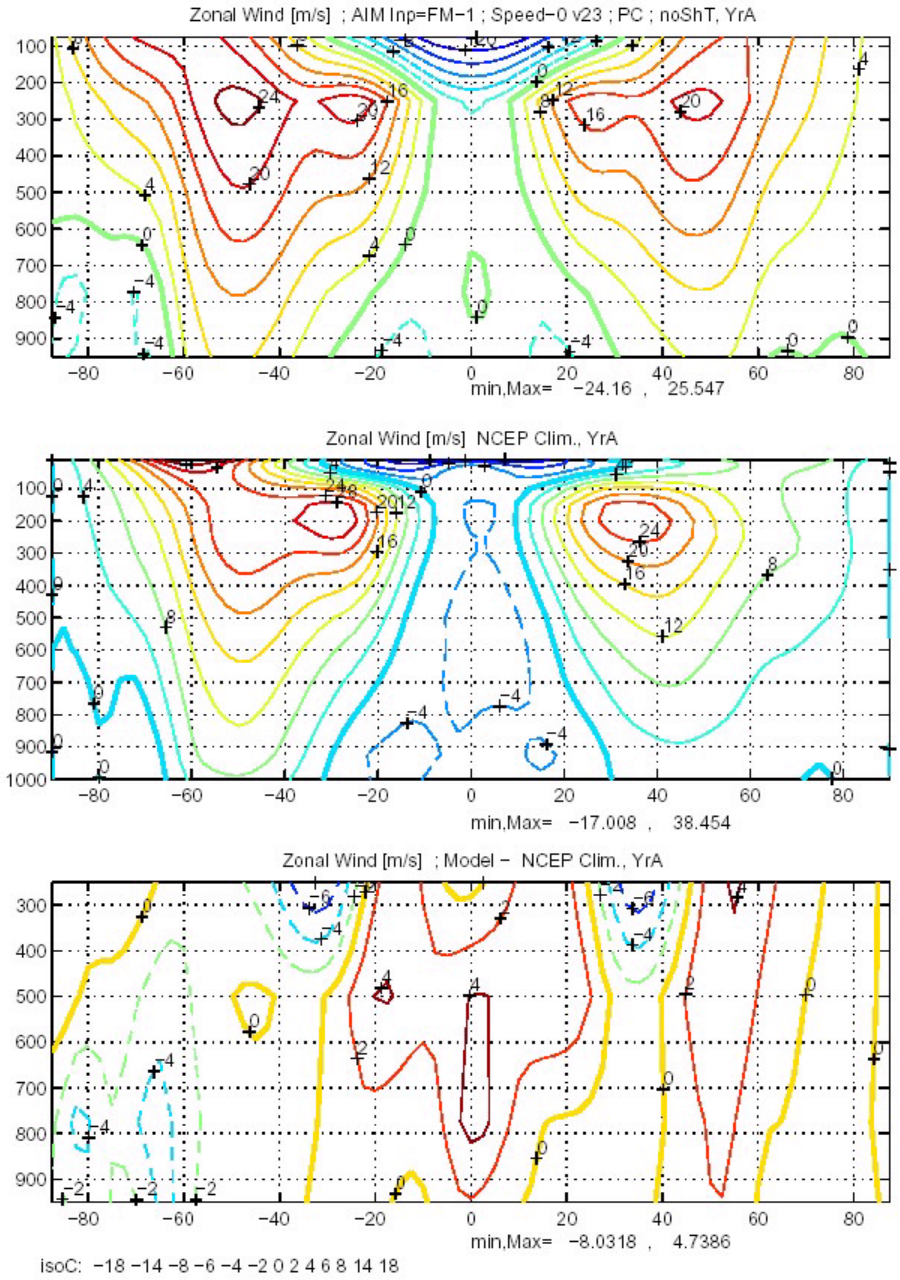


Figure 10: The zonal-average $U$ field obtained from a 5 year integration of the model (top - c.i.= $4ms^{-1}$) compared to the NCEP reanalysis (middle - c.i.= $4ms^{-1}$) and 'model' minus ''analysis' (bottom - c.i.= $2ms^{-1}$).

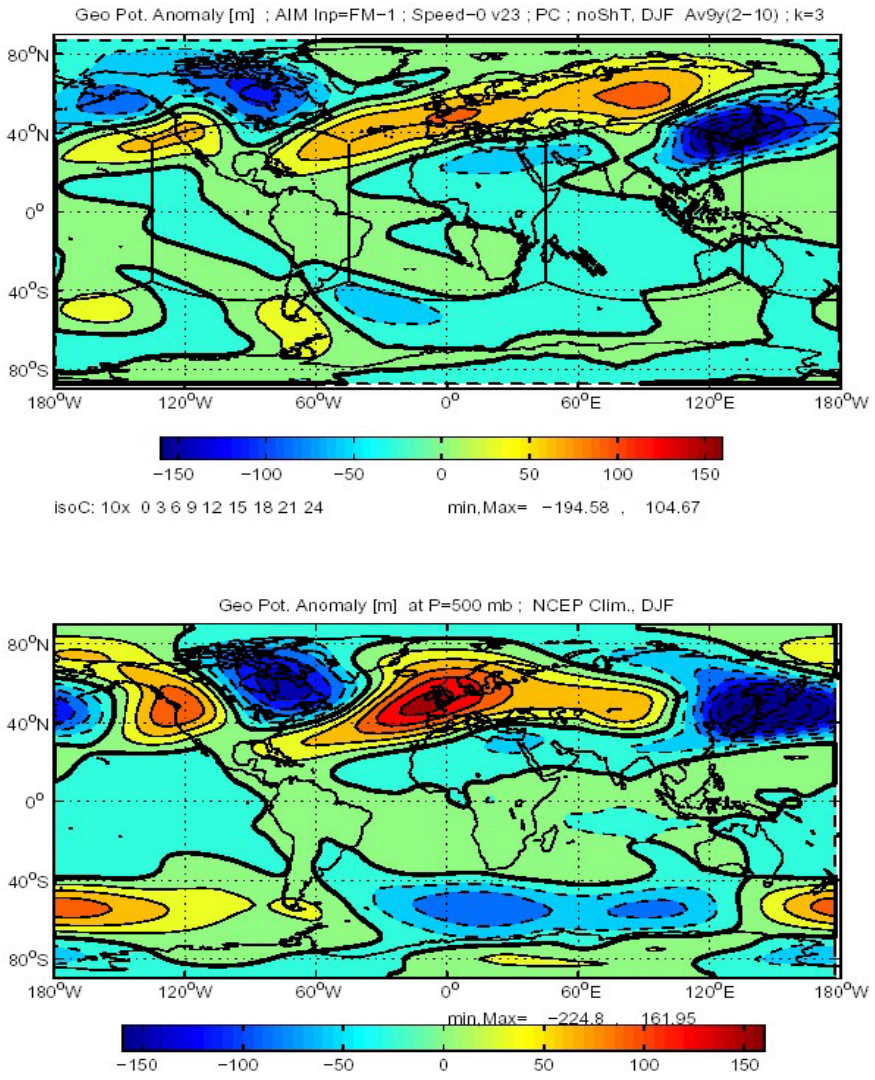


Figure 11: The geopotential height anomly of the 500mb surface in DJF in the model (top) and from the NCEP analysis (below): c.i.= $30m$.

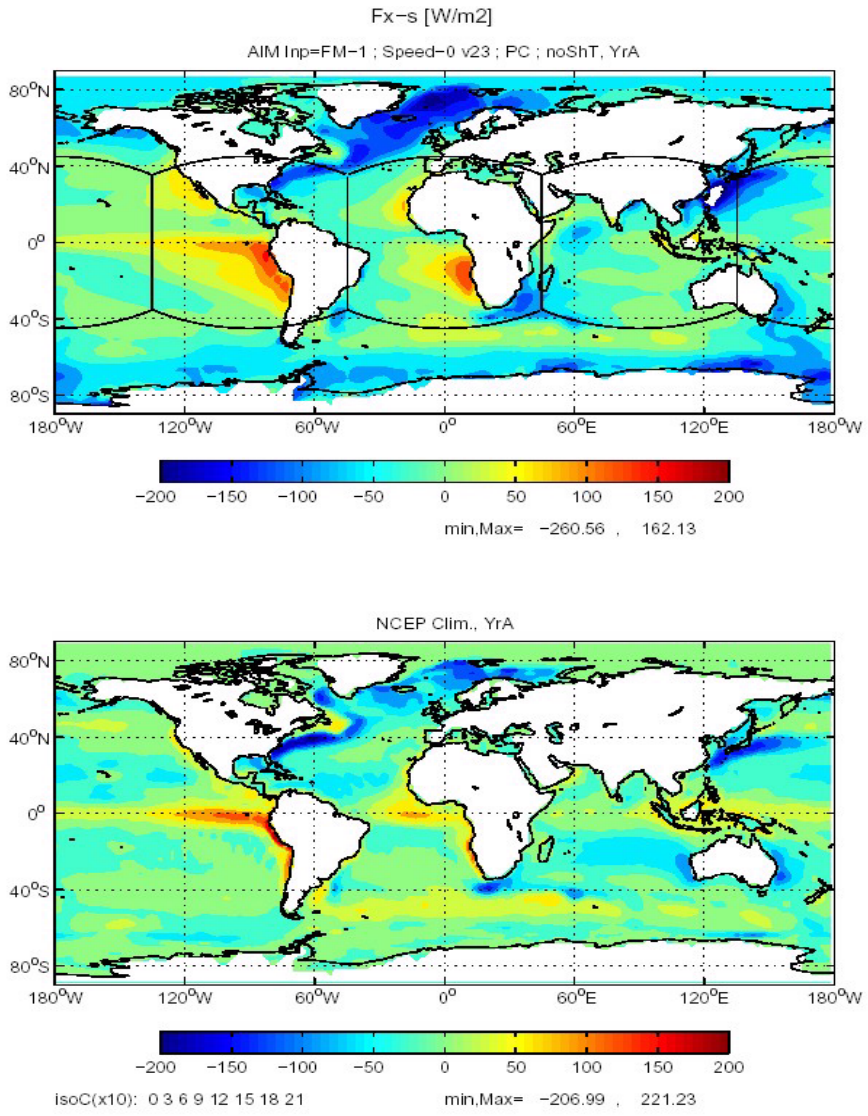


Figure 12: Net air-sea annual mean heat flux in the model (top) and from NCEP analysed fields (bottom). The color scale (same for both maps) is shown in the horizontal bar.

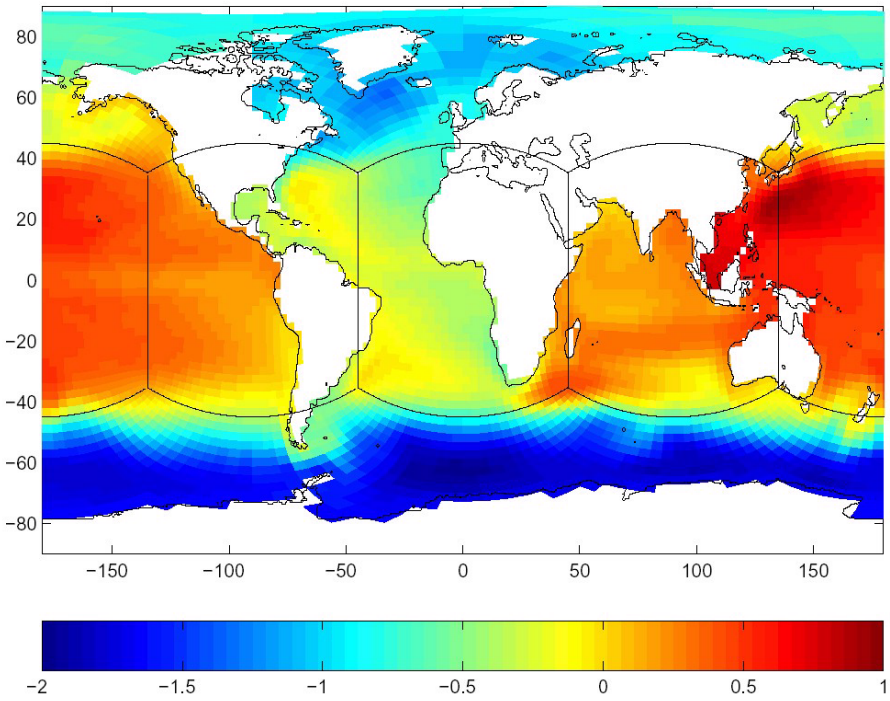


Figure 13: The sea surface height obtained from the cubed sphere ocean model - the colour scale is in metres.

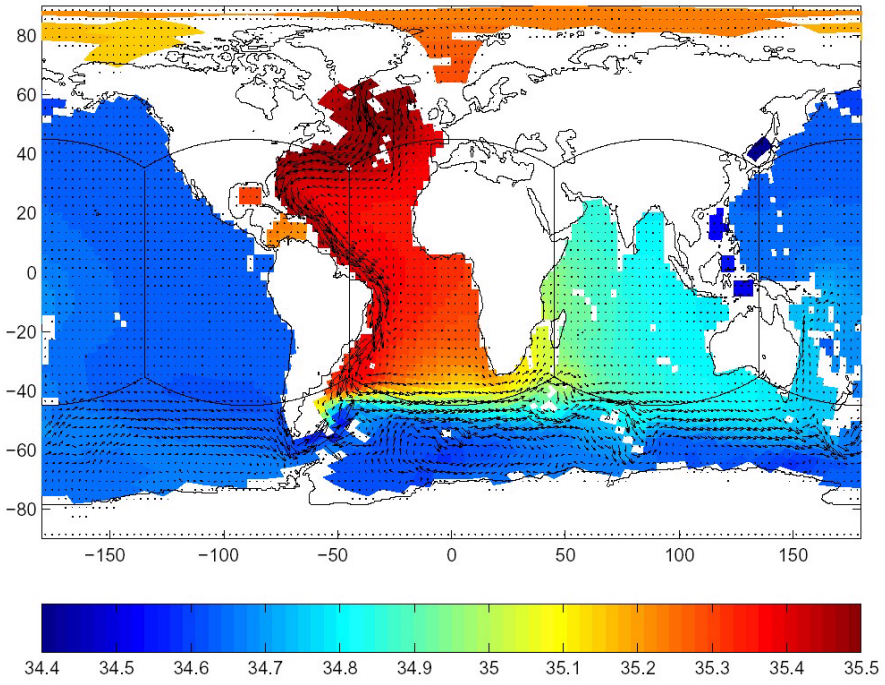


Figure 14: The flow at a depth of 2km (arrows) together with the salt distribution. Red is relative salty; blue is relatively fresh, as indicated on the colour scale.

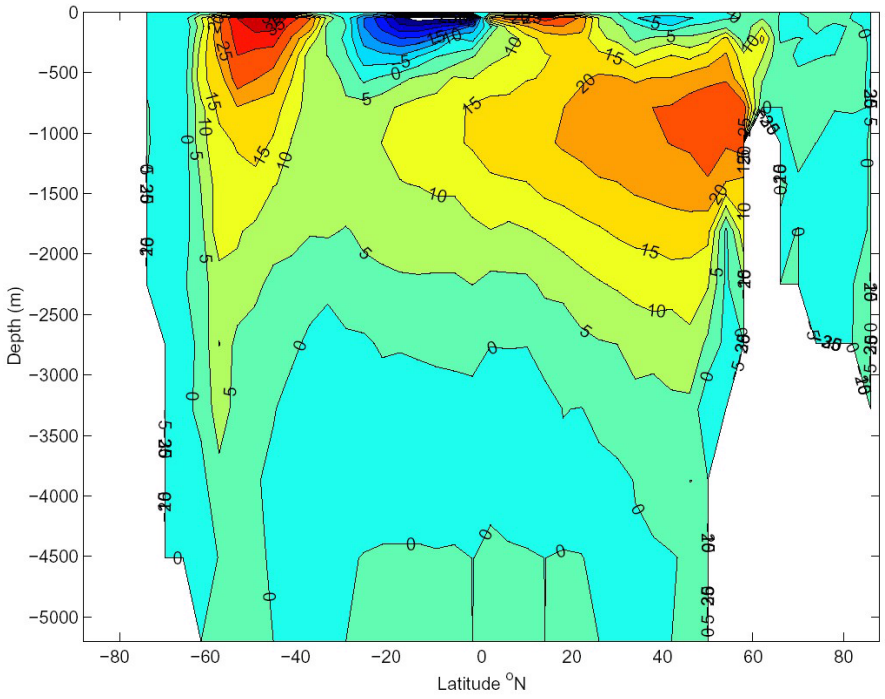


Figure 15: The global overturning streamfunction (in Sv) obtained from the cubed sphere ocean circulation model.